Electronic Supplementary Material (ESI) for Physical Chemistry Chemical Physics.

Supporting Information:

From nano to microcrystals: effect of different synthetic pathways on defects architecture in heavily Gd-doped ceria.

M. Coduri [1], M. Scavini [2,3], M. Pani [4,5], M. M. Carnasciali[4,6], H. Klein[7], C. Artini [4,8]

[1] ESRF – The European Synchrotron, 71, Avenue des Martyrs, 38000 Grenoble, France

[2] Dipartimento di Chimica, Università Degli Studi di Milano, via Golgi 19, 20133 Milano, Italy

[3] CNR-ISTM, Ist. Sci. & Tecnol. Mol., I-20133 Milano, Italy

[4] DCCI, Department of Chemistry and Industrial Chemistry, University of Genova, Via Dodecaneso 31, 16146 Genova, Italy

[5] CNR-SPIN Genova, Corso Perrone 24, 16152 Genova, Italy

[6] INSTM, Genova Research Unit, Via Dodecaneso 31, 16146 Genova, Italy

[7] Institut Néel, CNRS, Grenoble F−38042, France

[8] CNR-ICMATE, Via De Marini 6, 16149 Genova, Italy

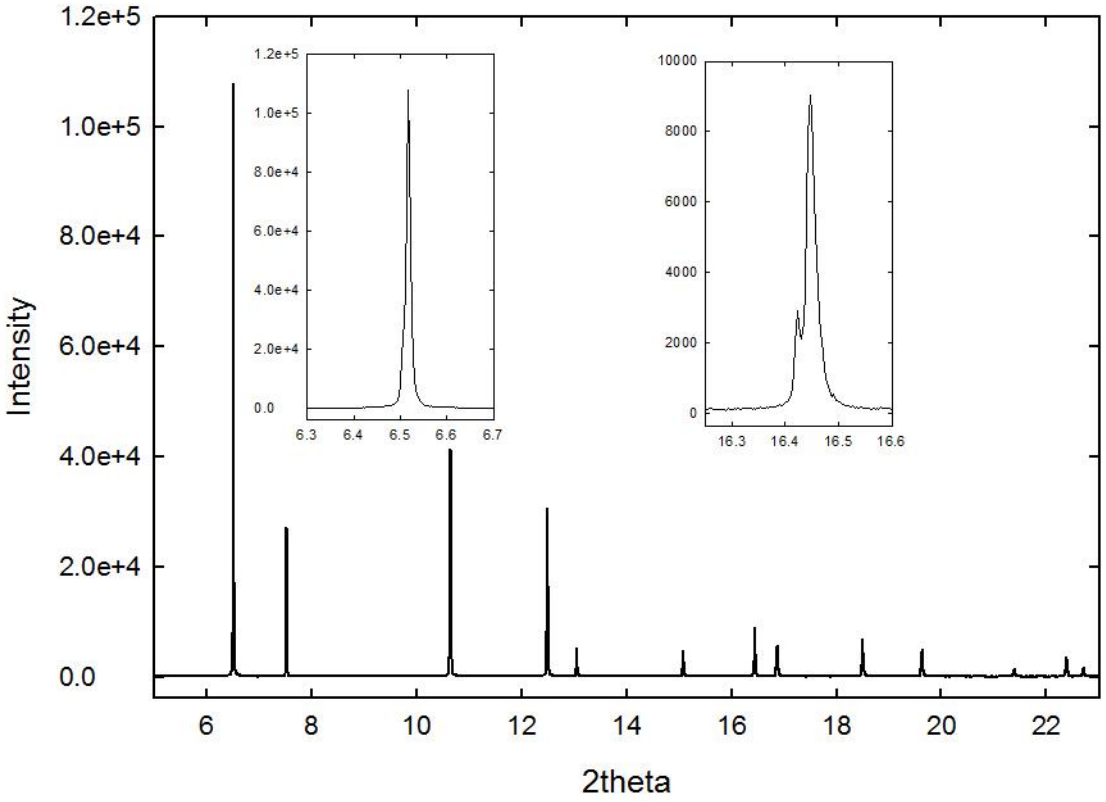

Figure SI1. Experimental XRPD pattern on a Gd-doped ceria sample collected at the ID22 high resolution beamline of the ESRF. Although a first glance suggests a monophasic sample, high angle data reveal sample inhomogeneity.

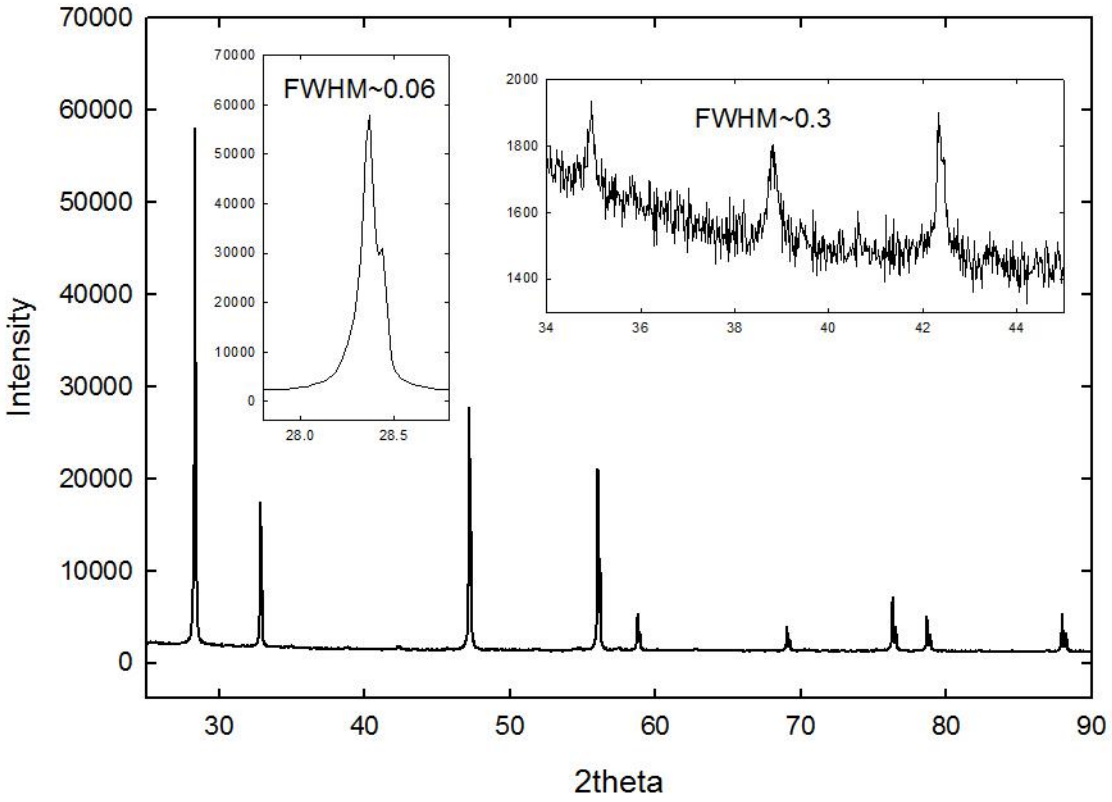

Figure SI2. Experimental XRPD pattern on a Gd-doped ceria sample collected on a Panalytical X'Pert Pro diffractometer. The profiles are very sharp and the width of the structure peaks is comparable to that of a

standard, even though some asymmetry is observed on the left-hand part of the main peaks. Superstructure peaks are broader than the main ones.

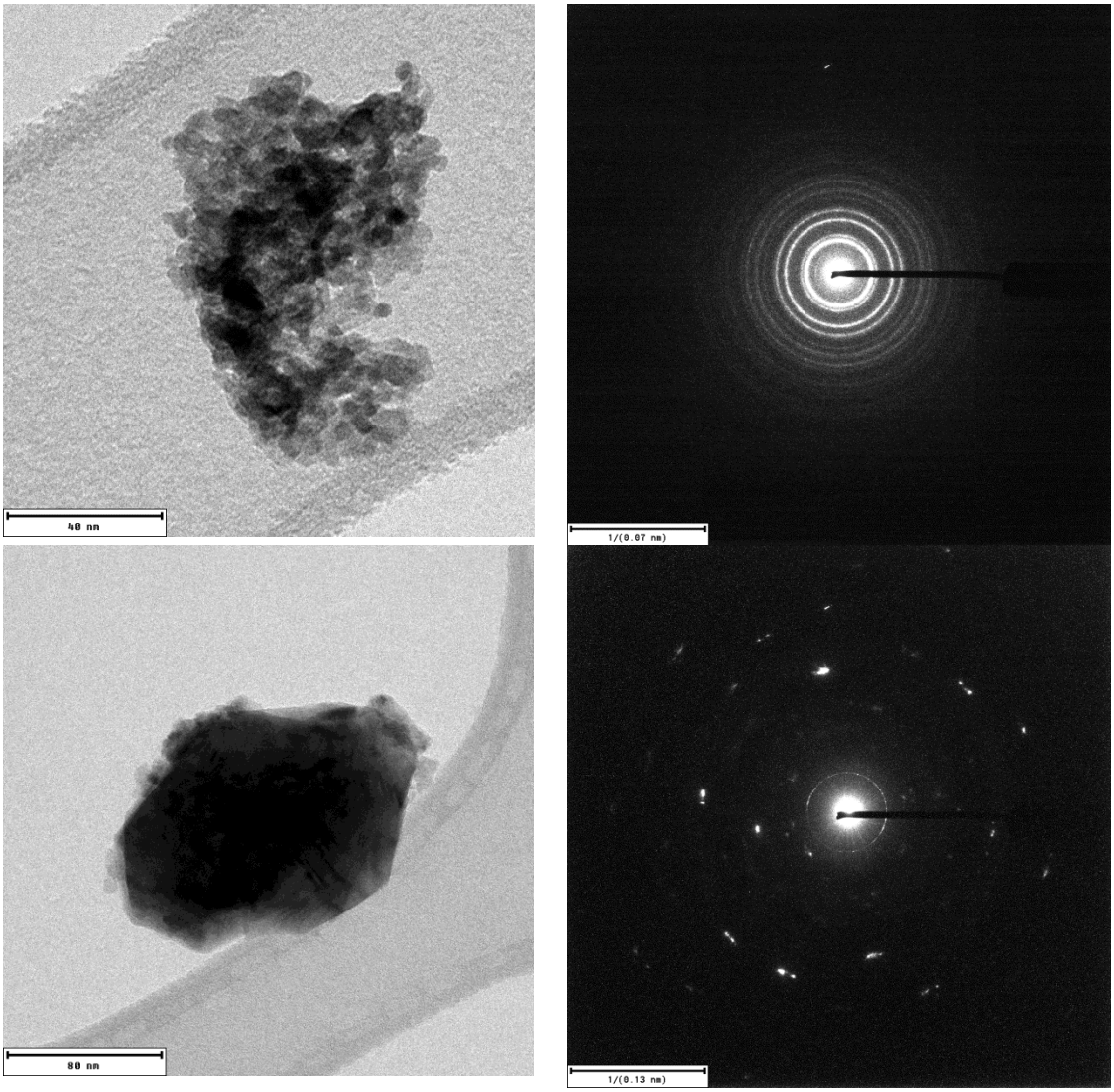

Figure SI3. TEM images recorded on sample with Gd313 composition, top: *sg*500, bottom: *sg*900. The corresponding electron diffraction pattern is displayed on the right, showing a high (*sg*500) and a poor (*sg*900) powder averaging, according to the different size distributions.

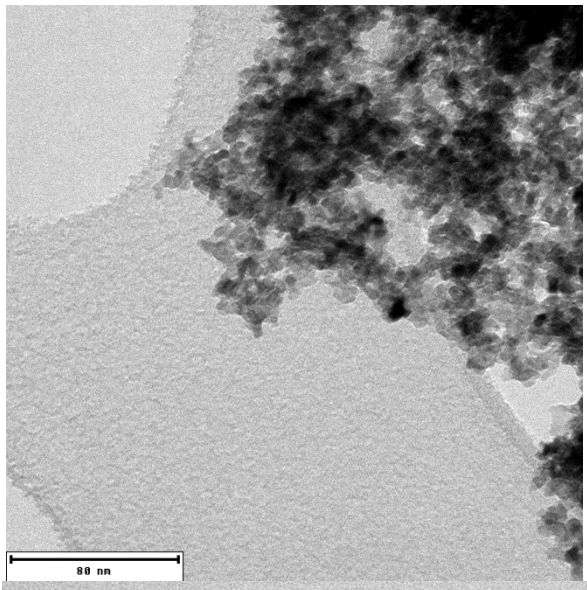
80 nm

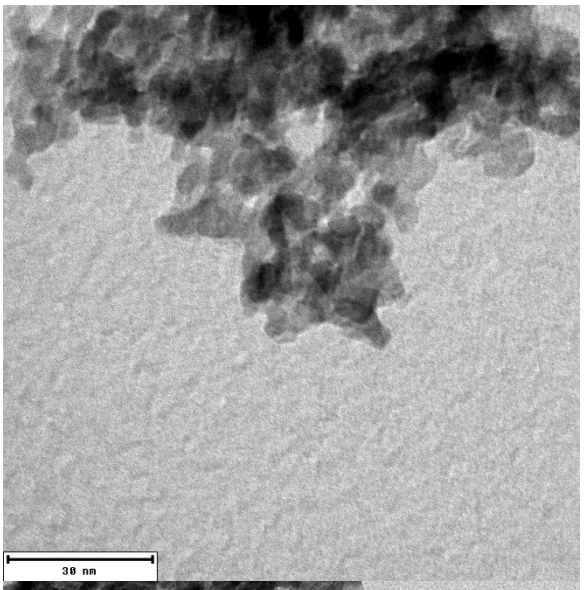
30 nm

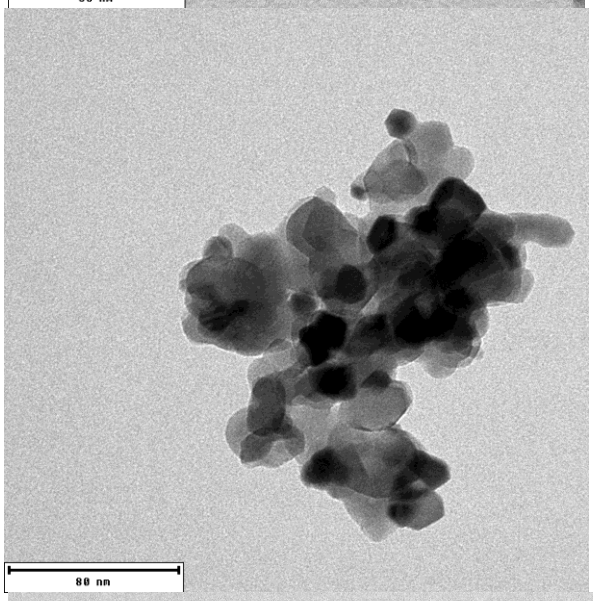
80 nm

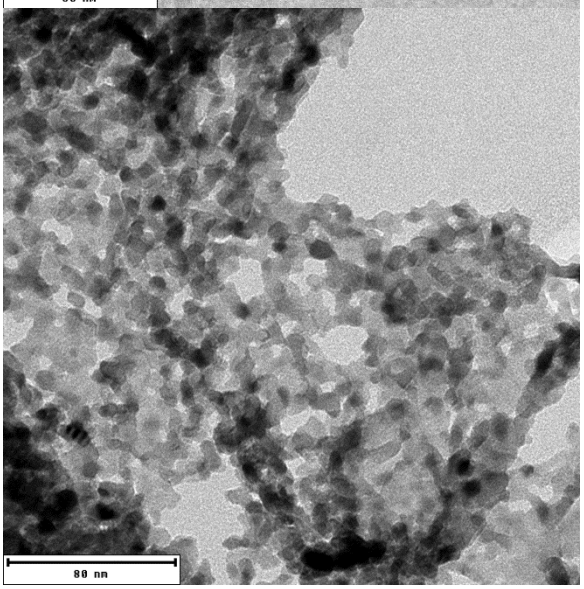
80 nm

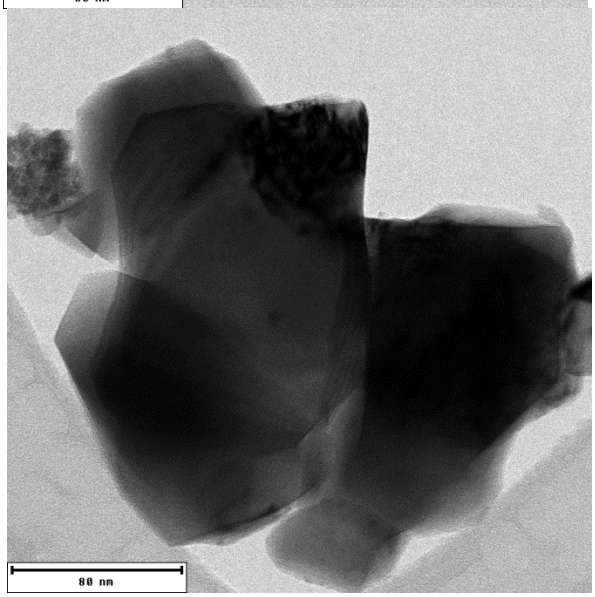
80 nm

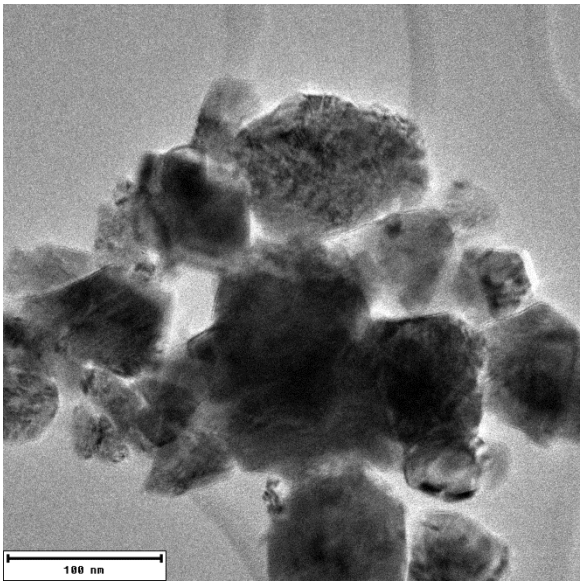
100 nm

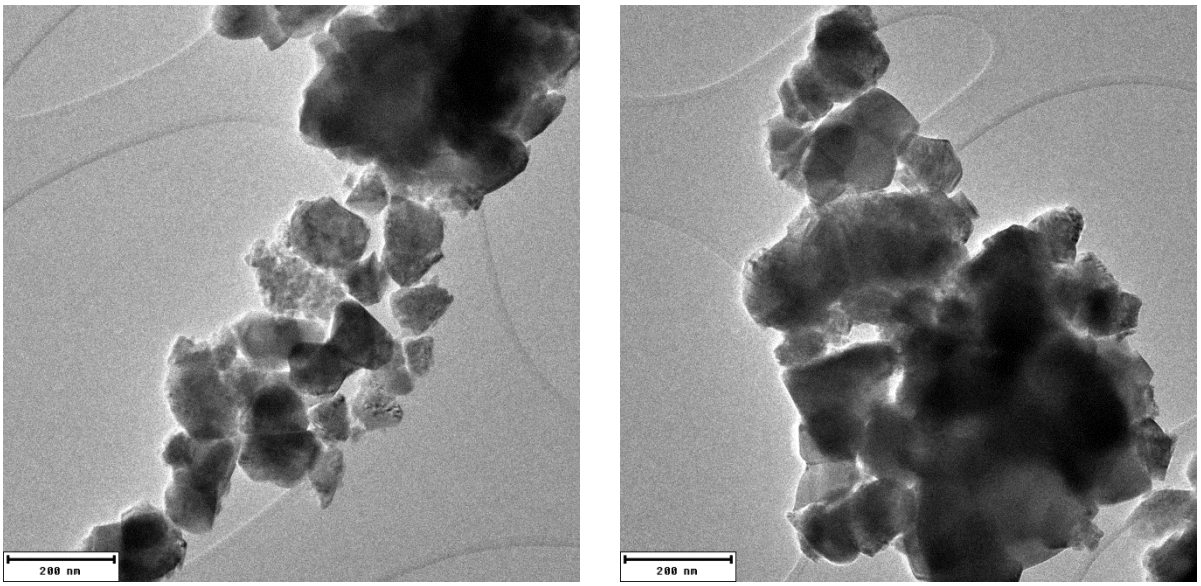

Figure SI4. TEM - Bright field images recorded, from top to bottom, on Gd313 *sg*500, Gd375 *sg*500, Gd313 *sg*900, Gd375 *sg*900.

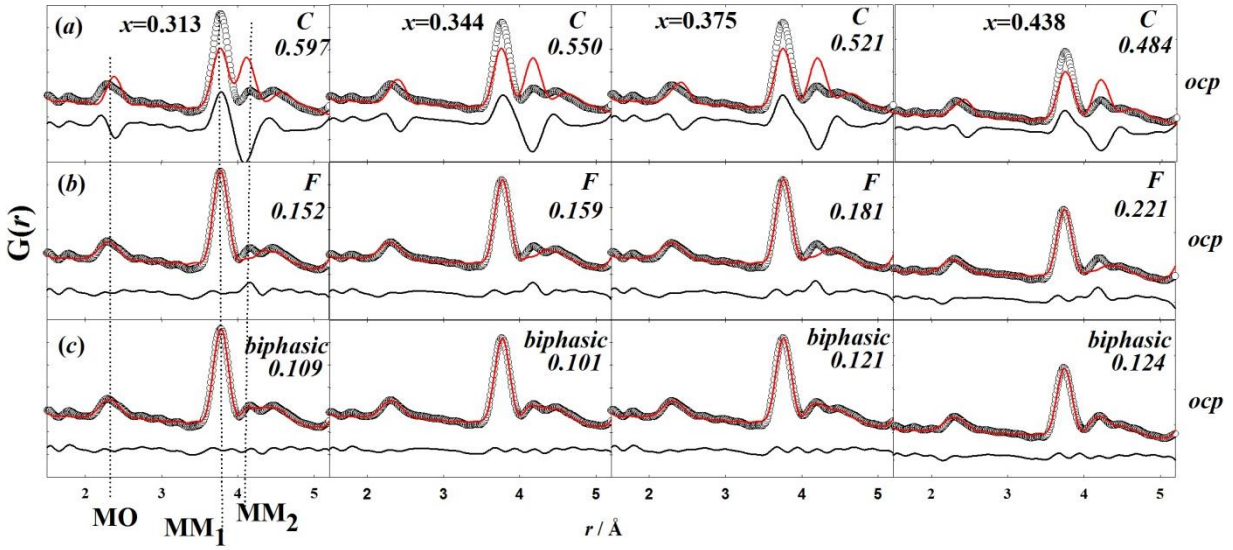

Figure SI5. Refinements of the local scale of PDF data for (*a*) single C-type, (*b*) single fluorite and (*c*) biphasic model for the four compositions investigated prepared via *ocp*. The fit residual Rw is indicated in each panel.

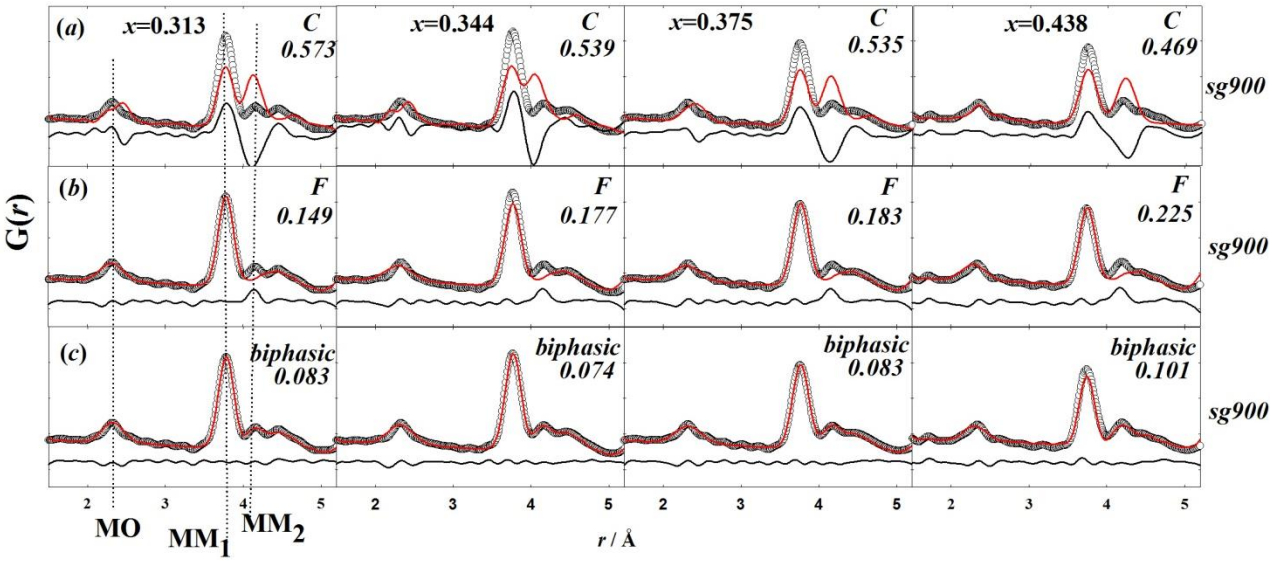

Figure SI6. Refinements of the local scale of PDF data for (*a*) single C-type, (*b*) single fluorite and (*c*) biphasic model for the four compositions investigated prepared via *sg*900. The fit residual Rw is indicated in each panel.

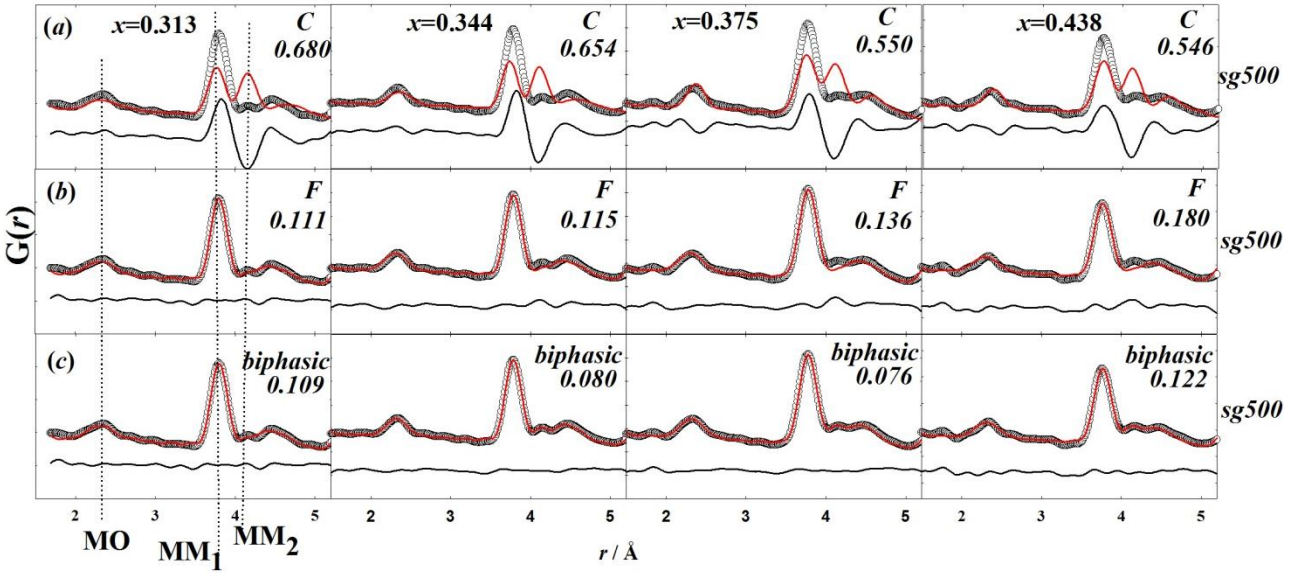

Figure SI7. Refinements of the local scale of PDF data for (*a*) single C-type, (*b*) single fluorite and (*c*) biphasic model for the four compositions investigated prepared via *sg*500. The fit residual Rw is indicated in each panel.